Formation of Nanometer-Scale Grooves in Silicon with a Scanning Tunneling Microscope

A. Kobayashi, F. Grey,* R. S. Williams, M. Aono

Grooves a few nanometers wide can be formed on a Si(111) surface with a scanning tunneling microscope when the tip is above a critical voltage. This may provide a promising approach to nanodevice fabrication. The dependence of the critical voltage on tunneling current, tip polarity, and tip material was studied with silver, gold, platinum, and tungsten tips. The results are consistent with field emission of positive and negative silicon ions. The variation of critical voltage with current is explained quantitatively by a simple tunneling equation that includes the effect of the contact potential between tip and sample.

The scanning tunneling microscope (STM) has been used to modify surfaces at the nanometer scale and to move single atoms (*1–3*). Modification of semiconductor surfaces is of particular interest for the fabrication of nanometer-scale quantum devices. At present, though, the physical mechanisms involved in such nanolithography are not well understood.

In a pioneering study, Becker *et al.* (*2*) made atomic-scale protuberances on Ge(111) by raising the bias of a W tip at constant tunneling current. This result was explained in terms of field emission of ions from the tip. Field-induced emission from the tip or sample has been proposed as a modification mechanism for other tip-sample combinations, including Au-Au (*4*), W-Pt (*5*), PtIr-Ag (*6*), and W-WSe_2 (*7*). However, Si(111) could not be modified in the same way as Ge(111), even for bias voltages up to 20 V and several nanoamperes (*2*). Atomic-scale modification of Si(111) has been achieved by another approach in which a W tip is moved nearly into point contact with the sample and a voltage pulse is applied to remove or deposit material (*3*). Although this process is field-dependent, detailed analysis is complicated because of chemical interaction between tip and sample. In this report, we describe an experiment in which nanometer-scale modification of Si(111) is achieved with an increase in the tip bias at constant current. In contrast to previous results, modification occurs even at relatively low voltages. Also, the tip remains in the tunneling regime, so the results can be analyzed with a simple model of electron tunneling.

We cleaned samples of *n*-type Si(111) wafers, resistivity 0.01 ohm cm, in ultrahigh vacuum (UHV) by annealing to 1150°C. Sharp Au, Ag, Pt, and W tips were prepared by electrochemical etching and were subsequently electron-bombarded in the UHV chamber of a commercial STM (VG Microtech, Uckfield, United Kingdom). Atomic-scale resolution of the Si(111) 7 × 7 reconstruction was obtained for all tips. To modify the surface, we increased the magnitude of the tip voltage, and the tip scanned over 60 nm at 50 nm/s. The same area was then imaged to detect modification. As the tip voltage increases in the modification scan, there is a critical voltage, V_c, above which Si is removed along the scanned line (Fig. 1).

The STM is sensitive to electronic effects as well as surface topography. To confirm that the observed modifications are indeed grooves, we imaged them at tip biases between +3 V and −3 V. Common contaminants, such as H and O, appear bright at some biases in this range (*8, 9*), and any deposited W, being a metal, should also appear bright. At all biases, however, the grooves appear dark, which confirms their topographical nature. This is illustrated in Fig. 2, where Si has been removed in an area about 4 nm across by application of a tip bias of 3.0 V and 0.25 nA for 2 s. Such small features can be made with the application of a bias slightly below V_c for a longer time than that for groove formation.

Well above V_c, protrusions are observed in the grooves of Fig. 1. These may be caused by material that has been deposited from the tip. Here, though, we only discuss the grooves formed at biases near V_c. The depths of the grooves cannot be estimated reliably, but they are greater than 5 Å (*10*). For the smaller features of Fig. 2, the profiles (Fig. 2, E and F) indicate a depth in the range of 2 to 4 Å below the average surface height. Such profiles correspond to the removal of Si adatoms and perhaps the Si bilayer below the adatoms. The bilayer is about 1.7 Å below the adatoms, and the next bilayer is 3.1 Å deeper (*11*).

More than ten tips were tested for each material. The value of V_c varied by less than 10% in all cases and no deterioration in the ability of a tip to modify was observed. This reproducibility indicates that the modification process does not depend sensitively on details of the tip geometry, which may vary from tip to tip. Hence, it should be adequate to model the tip-sample geometry over the modified area as a parallel-plate capacitor. A comparison of the radius of curvature of etched tips ($r > 500$ Å) with the tip-sample separation ($s \sim 10$ Å) supports this assumption. The applied electric field, F, is thus given to a first approximation by V/s, where V is the applied bias.

The average groove width increases as a function of tip bias at constant tunneling current (Fig. 3). If we take the width of the grooves as a measure of the amount of material that was removed, it is clear that the process is strongly voltage-dependent. In contrast, the current dependence of the groove width is weak (Fig. 3, inset). This rules out mechanisms such as electromigration (*12*), local melting (*13*), and electron beam–induced reactions (*14*), all of which vary strongly with current or total electron

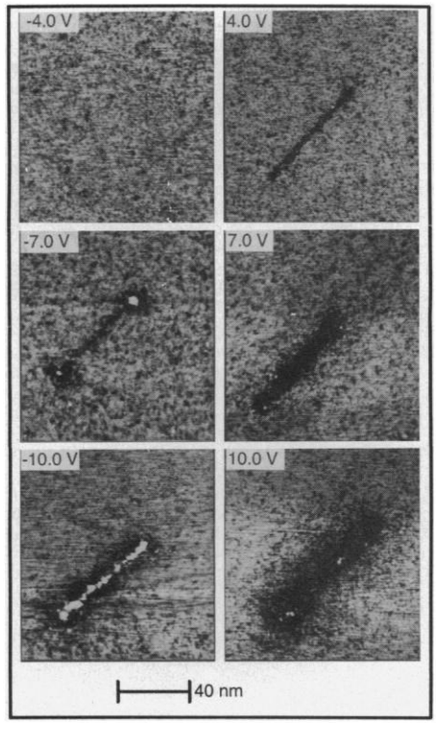

Fig. 1. Grooves formed on Si(111) by a W tip at both polarities of three selected biases. At this scale, the periodic structure of the Si(111) 7 × 7 reconstructed surface is not distinguishable. At negative bias, the critical voltage, V_c, is −4.75 V, so no modification is seen at −4 V. Well above V_c, at −10 V, a protrusion can be seen in the groove. The height scale is about 5.0 Å from black to white in all cases. Imaging conditions are −1.95-V tip bias and 0.25-nA tunneling current.

A. Kobayashi, F. Grey, M. Aono, Aono Atomcraft Project, ERATO, JRDC, 5-9-9 Tohkohdai, Tsukuba, Ibaraki 300-26, Japan.
R. S. Williams, Department of Chemistry and Biochemistry, University of California, Los Angeles, CA 90024–1569.

*To whom correspondence should be addressed.

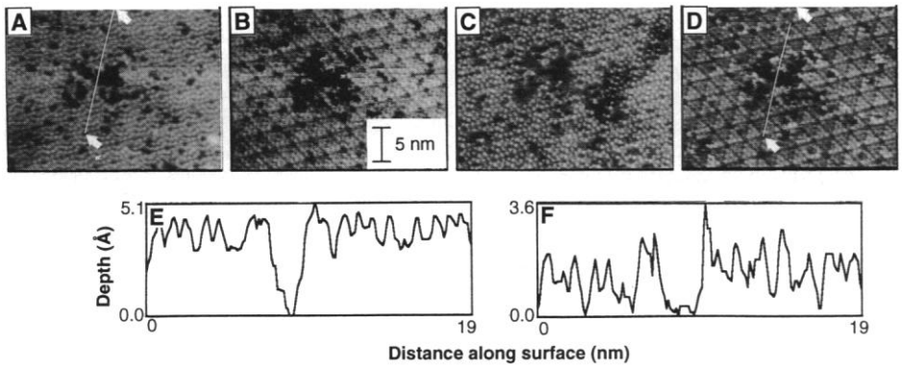

Fig. 2. An area from which Si has been extracted as described in the text, imaged at four different tip-bias conditions: (**A**) −1.95 V, (**B**) −0.98 V, (**C**) 1.15 V, and (**D**) 1.95 V. The tunneling current is 0.25 nA. At this scale, the periodic Si(111) 7 × 7 structure is apparent, and single Si adatoms can be distinguished. Defects caused by natural contamination can be seen only at certain biases, but the area at the center of the image, where extraction has occurred, appears dark at all biases, confirming its topographical nature. (**E** and **F**) Depth profiles of the modified area in (A) and (D), respectively (corresponds to the white lines indicated by arrows).

dose. The slow increase of groove width with the tunneling current, I, is consistent with field emission: in the tunneling regime, $s \propto -\log I$, and so $F \propto -1/\log I$ at constant bias.

We have measured V_c for four types of tips and both polarities in the current range 0.05 to 5 nA (Fig. 4). The main feature is that $V_c \propto \log I$. Because $s \propto \log I$, a constant slope in Fig. 4 means that V_c/s is constant; in other words, modification occurs at a current-independent critical field, F_c. This shows that groove formation is directly dependent on electric field, rather than on voltage, in contrast to electron-stimulated desorption of H on Si(111) (*15*), for which a fixed voltage threshold was observed. The result is consistent with field emission of ions (*16*); F_c is the critical field at which Si ions are emitted. A simple explanation for the observation of grooves at both polarities is that Si cations are emitted when the tip is biased negatively and Si anions are emitted at positive bias.

Concerning the dependence of V_c on tip material, a work function difference between tip and sample will generate a potential that affects sample or tip atoms (*17*). If the work function of the tip, Φ_t, is smaller than that of the sample, Φ_s, the result is a positive tip bias $(\Phi_s - \Phi_t)/e$, where e is the electron charge and Φ_s and Φ_t are measured in electron volts. The smaller Φ_t is, the larger the negative external bias that must be applied to the tip to overcome this contact potential and reach a given critical field. The reverse is true at positive applied bias. This trend is seen in Fig. 4: Ag and W, metals with relatively small work functions, have larger V_c at negative bias than Au or Pt. The reverse behavior is seen less clearly at positive bias for small currents.

The data can be analyzed by means of a simple expression for the tunneling current in the regime, where $eV \sim \Phi$, which is the case here (*18*)

$$j = \frac{e}{2\pi hs^2}\left\{(\Phi - eV/2)\exp\left[-\frac{4\pi s\sqrt{2m(\Phi - eV/2)}}{h}\right] - (\Phi + eV/2)\exp\left[-\frac{4\pi s\sqrt{2m(\Phi + eV/2)}}{h}\right]\right\} \quad (1)$$

In this equation, j is the current density, $\Phi = (\Phi_t + \Phi_s)/2$ is the average work function of tip and sample, h is the Planck constant, and m is the electron mass. To apply this expression, we introduce a tunneling area A, where $j = I/A$. The critical field, F_c, is assumed to be current-independent but depends on both tip material and polarity. It is related to V_c and the contact potential by

$$|F_c| = \frac{|(\Phi_s - \Phi_t)/e + V_c|}{s} \quad (2)$$

We fit Eq. 1 to the data by substituting for s from Eq. 2 and using standard values for the work functions of the tip materials and Si substrate (*16*, *19*). The only fitting parameters are F_c and A. Results are shown in Fig. 4 and the fit parameters are given in Table 1, along with the work functions of the tips and the variation of the nominal tip-sample separation, derived from Eq. 2, with V_c.

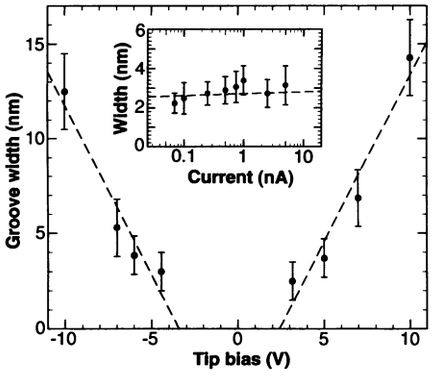

Fig. 3. Average groove width as a function of tip bias for a W tip at a constant tunneling current of 0.5 nA. Error bars indicate the variation observed along the length of a groove. Dashed lines are guides to the eye. The narrowest grooves are observed at V_c and are typically about 3 nm across, compared with the 2.7-nm edge length of the Si(111) 7 × 7 unit cell. (**Inset**) Groove width as a function of tunneling current for a tip bias of +4 V.

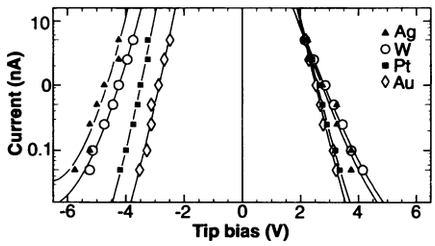

Fig. 4. Variation of V_c with tunneling current for four different tips: Ag, W, Pt, and Au. At a given current, each point represents the critical voltage at which groove formation begins. The curves are fits to the data as described in the text. Error bars on the data, left out for clarity, would be ±0.3 V.

Table 1. Results of a fit of a modified version of Eq. 1 to the data in Fig. 4. The data for each tip at either polarity were fitted separately. For each data set, the best fit values of the fit parameters F_c and A are given in the table. Error estimation is described in the text. The work functions that were used in the analysis are also listed, as well as the variation of the nominal tip-sample separation, s, over the range of current values for each data set.

Tip bias	Tip material	Φ_t (eV)	F_c (V/Å)	log (A) (Å^2)	s (Å)
−	Ag	4.3	0.31 ± 0.10	6.9 ± 2.5	12.0 to 16.7
−	W	4.5	0.39 ± 0.04	4.8 ± 0.8	8.9 to 12.6
−	Pt	4.8	0.31 ± 0.05	6.5 ± 1.4	10.4 to 13.5
−	Au	5.2	0.38 ± 0.08	4.8 ± 1.6	7.6 to 10.3
+	Ag	4.3	0.67 ± 0.16	1.0 ± 1.2	4.1 to 6.3
+	W	4.5	0.74 ± 0.04	0.4 ± 0.3	3.3 to 6.0
+	Pt	4.8	0.48 ± 0.03	1.7 ± 0.6	4.4 to 7.0
+	Au	5.2	0.48 ± 0.04	0.8 ± 0.4	3.7 to 5.9

All the values of F_c in Table 1 are much lower than the value of 3.8 V/Å that was found in field ion microscope (FIM) experiments for positive Si ions (*17*). Similar reductions of F_c in STM geometry have been seen before (*3, 4, 5*). This effect has been discussed in terms of the overlap of image potentials of tip and sample, which reduces the barrier to field emission (*4, 13*). Recent calculations (*20, 21*) show that, in STM geometry, ions can be emitted at much lower fields than in FIM studies, consistent with the relatively small F_c values determined here.

The F_c values at negative bias are the same, within errors, for all tips, which agrees with the simple picture that F_c is an intrinsic property of the Si, independent of the tip material. There is more scatter at positive bias; but the tip-sample separation is also considerably smaller, so the effects of interaction with the tip may be more pronounced. Although anion emission cannot normally be observed in FIM studies because of the large electron currents generated at negative tip bias (*21*), recent theoretical studies support the view that anion emission should occur at critical fields similar to those for cations (*13, 20, 21*).

The values of A are of the order 1 to 10 $Å^2$ at positive bias but are considerably larger at negative bias. However, it would be overly simplistic to interpret these differences solely in terms of variations of the tunneling area. For example, in more detailed treatments of the tunneling equation at low bias (*22*), other parameters enter into the exponential prefactor, such as the electronic density of states of the emitter. To further investigate such effects, a more detailed theory of tunneling is needed in the medium voltage regime where $V \sim \Phi$. We note that in the fitting procedure, A couples strongly to the values of Φ_t and Φ_s. This is a large source of uncertainty because the quoted values of work functions vary considerably (*19*). The values that we used for the metal tips were based on contact-potential measurements that related to a standard value for W (*19*). For Si, a standard value of 4.8 eV was used (*16*). The errors in Table 1 include a ±0.2 eV variation in the work function values.

We stress the importance of tip preparation in achieving reproducible results. For W tips that were not electron-bombarded, groove formation was not reproducible and often did not occur even at tip biases up to 10 V. A possible explanation is the presence of an oxide layer several nanometers thick on the tips (*23*). The field at the sample may be substantially reduced by the presence of this dielectric film near the end of the tip. Electron bombardment effectively removes the oxide over a large area. We note that Au tips can modify the surface in a reproducible way without electron bombardment, presumably because Au is comparatively inert. Thus, we suggest that the discrepancy between our results and earlier attempts (*2*) to modify Si(111) is attributable to tip preparation. This is a controversial hypothesis that deserves further study because it may be important in other STM nanomodification experiments.

With research based on our results, it has recently been shown that single Si atoms can be removed by a brief pulse near the critical voltage (*24*). Such single-atom modification is a probabilistic event because field emission is a thermally activated process. Modification on the scale of the grooves in Fig. 1 may ultimately be of greater technological significance, though, because it is highly reproducible.

REFERENCES AND NOTES

1. J. A. Stroscio and D. M. Eigler, *Science* **254**, 1319 (1991).
2. R. S. Becker *et al.*, *Nature* **325**, 419 (1987).
3. I.-W. Lyo and P. Avouris, *Science* **253**, 173 (1991).
4. H. J. Mamin, P. H. Guethner, D. Rugar, *Phys. Rev. Lett.* **65**, 2418 (1990).
5. S. E. McBride and G. C. Wetsel, *Appl. Phys. Lett.* **59**, 3056 (1991).
6. J. P. Rabe and S. Buchholz, *ibid.* **58**, 702 (1991).
7. T. Schimmel *et al.*, *ibid.*, p. 1039.
8. I.-W. Lyo, P. Avouris, B. Schubert, R. Hoffmann, *J. Phys. Chem.* **94**, 4400 (1990).
9. J. Boland, *J. Vac. Sci. Technol. B* **9**, 764 (1991).
10. With this STM, the vertical range is determined automatically by a prescan of a small region of the desired scan area. Because the Si(111) surface is very flat, the range is typically limited to about 5 Å. Attempts to image atomic structure inside the grooves were unsuccessful.
11. K. D. Brommer, M. Needels, B. E. Larson, J. D. Joannopolous, *Phys. Rev. Lett.* **68**, 1355 (1992).
12. D. M. Eigler *et al.*, *Nature* **352**, 600 (1991).
13. T. T. Tsong, *Phys. Rev. B* **44**, 13703 (1991).
14. E. A. Dobisz and C. R. K. Marrian, *J. Vac. Sci. Technol. B* **9**, 3024 (1991).
15. R. S. Becker, G. S. Higashi, Y. J. Chabal, A. J. Becker, *Phys. Rev. Lett.* **65**, 1917 (1990).
16. T. T. Tsong, *Atom-Probe and Field Ion Microscopy* (Cambridge Univ. Press, Cambridge, 1990.
17. R. Gomer, *IBM J. Res. Dev.* **30**, 428 (1986).
18. J. G. Simmons, *J. Appl. Phys.* **34**, 1793 (1963).
19. D. E. Gray, Ed. *American Institute of Physics Handbook* (McGraw-Hill New York, ed. 3, 1972).
20. N. D. Lang, *Phys. Rev. B* **45**, 13599 (1992).
21. N. M. Miskovsky, C. M. Wei, T. T. Tsong, *Phys. Rev. Lett.* **69**, 2427 (1992).
22. J. Tersoff and D. Hamann, *Phys. Rev. B* **31**, 805 (1985).
23. J. Garnaes, F. Kragh, K. A. Morch, A. R. Tholen, *J. Vac. Sci. Technol. A* **8**, 441 (1990).
24. H. Uchida, D. H. Huang, F. Grey, M. Aono, unpublished data.

25. We thank H. Rohrer, T. T. Tsong, and R. Synder for discussions and H. Uchida and D. H. Huang for allowing us to refer to their results before publication.

8 June 1992; accepted 13 January 1993

Boundary Layer Profiles in Plasma Chemical Vapor Deposition

David S. Green, Thomas G. Owano, Skip Williams, David G. Goodwin, Richard N. Zare, Charles H. Kruger*

A nonlinear optical spectroscopy based on degenerate four-wave mixing has made possible direct measurements of species temperature and concentration profiles through the boundary layer of a reactive plasma at atmospheric pressure. Spectra were obtained for CH and C_2 radicals over a range of conditions including those for the plasma chemical vapor deposition of diamond films. Numerical simulations based on a one-dimensional stagnation-point flow model are in good agreement with the measurements. The CH mole fraction is shown to rise and fall as a function of distance from the substrate, which is compelling experimental evidence for the complex chemistry that is occurring in the plasma boundary layer.

Plasmas find a wide range of applications from light sources to materials synthesis and even the development of controlled fusion. Yet the contribution of plasmas to emerging technologies relies on our ability to characterize what is among the harshest of chemical environments. The intense luminosity along with the rapidly changing chemistry, temperature, pressure, and velocity challenge our ability to make meaningful measurements and to model such systems. Diagnostics are required to provide information about neutral and ionized species, electron density, and energy in the plasma. Furthermore, the implementation of such diagnostics must be nonintrusive, species- and state-selective, sensitive, and capable of high spatial and temporal resolution. We report the use of resonant degenerate four-wave mixing (DFWM) (*1, 2*) to probe the boundary layer chemistry of an atmospheric-pressure radio-frequency, inductively coupled plasma. As a representative system, we used an industrial-scale reactor and made in situ measurements of the temperature and concentration of CH

D. S. Green, S. Williams, R. N. Zare, Department of Chemistry, Stanford University, Stanford, CA 94305.
T. G. Owano and C. H. Kruger, High Temperature Gasdynamics Laboratory, Department of Mechanical Engineering, Stanford University, Stanford, CA 94305.
D. G. Goodwin, Division of Engineering and Applied Science, California Institute of Technology, Pasadena, CA 91125.

*To whom correspondence should be addressed.